Micromachined high gain wideband antennas for wireless communications

Sumanth K. Pavuluri, Changhai Wang and Alan J. Sangster
Heriot Watt University
Edinburgh, EH14 4AS, UK

1. Introduction

The seemingly insatiable and growing demand for compact, multi-function, multi-frequency electronic systems for communications and other applications, is continuing to drive the search for devices offering more and more bandwidth. There is growing need for broadband high gain communication systems in the X band range of frequencies (8 - 12 GHz) for terrestrial broadband communications and networking as well as for radar applications. Similarly, direct broadcast satellite (DBS) and various other applications in the K_u band (10 - 14 GHz) such as radio astronomy service, space research service, mobile service, mobile satellite service, radio location service (radar), amateur radio service, and radio navigation may require embedded antenna systems at different bands. It would be ideal if efficient, broadband and cost effective planar microstrip based antenna and antenna array devices could be designed to provide coverage of all these bands. In addition systems aimed at UWB (Ultra Wide Band) operation need efficient very wideband antenna devices.

For these high frequency systems, compact size and high performance can usually be achieved by fabricating the antenna onto a low dielectric constant material and integrating it with the remaining circuitry implemented on a high dielectric constant substrate in neighbouring regions in the same package. This trend has serious implications for antennas, where these are required to be embedded within the system package, such as a mobile phone. Systems operating in the microwave and millimetre-wave frequency bands offer the possibility of high levels of integration of individual devices in high density layouts. The most compact circuit designs are invariably achieved by employing high dielectric constant substrates, but this is a requirement which is essentially incompatible with the needs of an embedded planar antenna. Such antennas radiate most efficiently when fabricated onto substrates which exhibit low dielectric constant (Papapolymerou et al., 1998). While it is not impossible to fabricate microstrip or coplanar circuits, together with planar antennas on the same high permittivity silicon substrate, antenna gain and efficiency will inevitably be very poor.

Various schemes have been suggested, in recent years, aimed at overcoming the opposing substrate requirements of circuits and antennas. These largely involve the use of layered materials with high and low permittivities in adjacent layers (Chen, 2008). However such

methods tend to be of quite limited versatility and the trend now is toward selective removal of substrate in the vicinity of the antenna. This can be done by, for example, bulk micromachining an air gap between the planar antenna (usually a conducting patch) and the ground plane (Koul, 2007). The advantages of doing so are as follows:

- Lower effective dielectric constant, hence wider circuit dimensions
- Ease of fabrication and relaxed dimensional tolerances
- Lower attenuation
- Enhanced radiation efficiency in case of antennas
- Eliminating surface waves

Micromachining technology continues to develop, and it is being applied in new ways to embedded antennas to improve their performance. The use of selective lateral etching based on micromachining techniques to enhance the performance of rectangular microstrip patch antennas printed on high-index wafers such as silicon, GaAs, and InP have been developed in the past decade. A novel polymer micromachining based method for achieving high performance, cost effective antennas is described in this chapter.

2. Micromachined antennas

Over the last decade several micromachining techniques have been developed for producing microwave wave and millimeter wave antennas. Devices using these procedures have achieved high performances compared to the conventional patches printed on to relatively high dielectric constant substrates. Various micromachining methods that have been implemented recently are listed in the following sections.

2.1 Silicon micromachining

Silicon micromachining has been employed to fabricate a patch antenna wherein, the silicon material was removed laterally underneath it thus producing a cavity that consists partly of air and partly of substrate (Papapolymerou et al., 1998, Hou et al., 2008, Ojefors et al., 2006, Kratz and Stenmark, 2005). Examples with both equal and unequal thicknesses of air and substrate have been implemented. The micromachined antenna configuration consisted of a rectangular patch centred over the cavity, sized according to the effective index of the cavity region, and fed by a microstrip line. To produce the mixed substrate cavity region, silicon micromachining was used to laterally remove the material from underneath the patch resulting in two separate dielectric regions of air and silicon. The amount of silicon removed varied from 50 to 80% of the original substrate thickness underneath the patch. A cavity model was used to estimate the effective refractive index value below the patch. The walls of the hollowed cavity tend to be, slanted owing to the anisotropic nature of the chemical etching, and this has to be allowed for in the modelling. This antenna has been shown to exhibit superior performance over conventional designs with the bandwidth and the efficiency having been increased by as much as 64% and 28%, respectively.

2.2 Polymer micromachining

Thick photoresist patterning processes can be used to fabricate an air suspended patch antenna either with supporting metallic posts or polymer posts. Antenna structures at

different frequency bands require different air cavity thickness to achieve optimum antenna performance and better impedance matching. Photoresist based polymers such as SU8 and THB151N can be used to obtain ultra thick supporting posts and can also be used as moulds for electroplating metal posts. Various polymer micromachining methods have been implemented in the past (Ryo-ji and Kuroki, 2007). A CPW fed post supported patch antenna has been fabricated on a Corning 7740 glass substrate which had a thickness of 800 μm and a dielectric constant of 4.6. Copper was used for metallization. The feed line of the antenna was patterned with the thick photoresist of AZ9260 and a two-step coating process was performed to form the posts of the antenna with a thick photoresist of THB151N. A simulated antenna gain in the range of 5.6 dBi to 9.0 dBi and the radiation efficiency varying from 92.8 % to 97.4 % were demonstrated for single patch antennas. In the case of a 2 × 1 array patch antenna, the simulated antenna gain and the radiation efficiency were from 5.8 dBi to 11.2 dBi and from 93.6 % to 95.3 %, respectively.

SU8, a widely used negative tone photoresist, has been used to fabricate an elevated patch antenna with micromachined posts of around 800 μm of height. (Pan et al., 2006; Bo et al., 2005) have successfully demonstrated an air-lifted patch antenna fabricated using surface micromachining technology. Both metal posts and polymer posts were used to provide mechanical support, as well as electrical excitation. A -10 dB bandwidth of 7%, centred at 25 GHz, was obtained. The proposed structure is superior to the conventional patch in terms of bandwidth, efficiency and lower side lobe level. While the traditional patch antenna directly printed on substrate usually gives a 3%-5% bandwidth and 70%-80% radiation efficiency, the proposed elevated patch will double the fractional bandwidth and gives a theoretical 97% radiation efficiency. This is achieved by eliminating the substrate loss. Low permittivity spin-on dielectric substrates are efficient for guiding microwaves and millimetre waves (Wang et al., 2005) and they have been used for microwave filters to improve the insertion loss of devices fabricated on silicon substrates (Leung et al., 2002).

2.3 Millimeter wave antennas using low permittivity dielectric substrates and micromachining

Antennas using low permittivity dielectric substrate have wider impedance bandwidth and higher gain when compared with those using ceramic dielectric substrates. Tong et al have presented the simulation and measurement of millimeter-wave CPAs (Coplanar patch antennas) using spin-on low-k dielectric substrate (Tong et al., 1995). The antenna composes of a gold ground plane at the bottom, two layers of BCB dielectric substrate (ε_r = 2.7 and $tan\delta$ = 0.002 @ 20GHz) in the middle and a CPA pattern on the top. The total thickness of the BCB layer is 30 μm. Fluid state BCB is spun onto a 3-inch ground plane coated silicon wafer. The deposition technique is similar to the commonly used photoresist coating technique and the metal CPA pattern is evaporated onto the BCB dielectric layer. The thicknesses of the ground plane and the CPA pattern are both about 1.5 μm. The simulated and measured impedance bandwidths are about 1.2% and 2.6% respectively. The measured resonant frequency of the antenna is 38.3 GHz. Micromachining techniques employing closely spaced holes have been used underneath a microstrip antenna on a high dielectric-constant substrate to synthesize a localized low dielectric-constant environment (ε_r = 2.3) (Gauthier et al., 1997). The holes are drilled using a numerically controlled machine (NCM) and extend at least 3.5 mm from the edge of the antenna in all directions and occupy the full substrate

height. The measured radiation efficiency of a microstrip antenna on a micromachined substrate (Duroid 6010, ε_r = 10.8) increased from 48.3% to 73.3% at 12.8 – 13.0 GHz (including the loss with a 3.3 cm long feed line).

## 2.4 Integrated chip-size antennas using laser micromachining

Integrated laser micromachined antennas on glass substrates are compact due to reduced size and owing to the relatively high dielectric constant. Mendes et al have reported an on-chip integrated, folded short-patch antenna (Mendes et al., 2006). It consists of three horizontal metal sheets that are electrically connected by two vertical metal walls. All this is embedded in a glass substrate having defined electrical permittivity and dielectric losses. The antenna was designed to operate at 5.1 GHz, a frequency chosen to be inside the 5 – 6 GHz ISM band. The fabricated antenna has dimensions of 4mm×4mm×1mm, a measured operating frequency of 5.05 GHz with a bandwidth of 200 MHz at the return loss of −10 dB and a simulated radiation efficiency of 60%. A method of applying laser micromachining technologies to fabricate a compact, high performance and low-cost 3D monopole antenna was proposed by Huang et al (Huang et al., 2005). The coplanar waveguide (CPW) fed configuration was used owing to its simple structure, wide bandwidth, and the ability of multi-band operation.

2.5 LTCC micromachining

LTCC multilayer technology can be used to build up antenna arrays because it provides the necessary degree of vertical integration for the high-density microwave circuit and a packaging solution such as SIP (System in Package) (Wolff, 2007, Baras and Jacob, 2008, Wi et al., 2007). To optimise the material properties by reducing the relative permittivity of LTCC, a material modulation procedure based on punching air holes into the substrate is performed. Thereby, the relative permittivity of the material is replaced by the effective relative permittivity ε_r of the modulated material (Schuler et al., 2003).

3. Antenna design and modelling

A compact planar antenna which is eminently suitable for embedding within integrated electronic systems is the patch antenna shown in Fig. 1. This type of antenna can be excited in one of four ways (Pozar, 1992, James and Hall, 1989, Bahl and Bhartia, 1980): (a) directly from a microstrip line, (b) electromagnetically from a buried line, (c) directly from a coaxial line probe, and (d) electromagnetically by means of a slot. Of these only (d) permits the implementation of multi-layered formats and consequently the section is directed toward assessing this geometry in relation to the micromachining of such structures.

(a) Microstrip feed

(b) Buried line feed

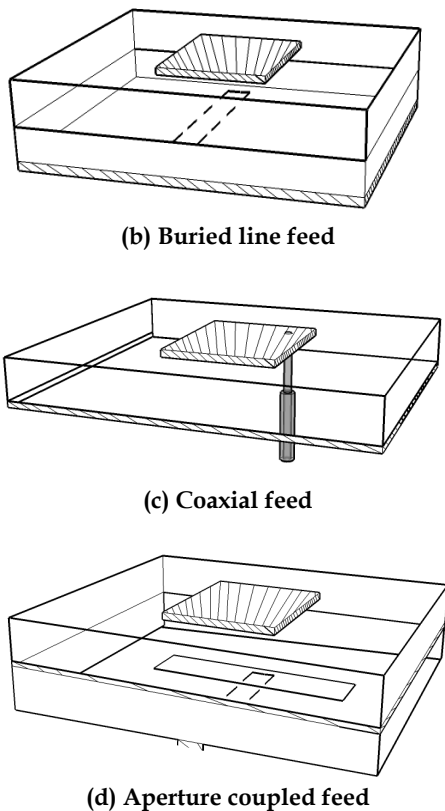
(c) Coaxial feed
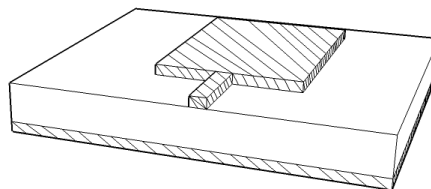
(d) Aperture coupled feed

Fig. 1. Illustration of feeding methods for microstrip antennas.

High gain and wideband micromachined microstrip and aperture fed stacked patch antenna devices have been designed and are described in the following sections. The antenna devices have been modelled using an electromagnetic simulation package. The structures are fabricated in layers and then assembled to obtain 3D devices. The detailed fabrication and assembly processes will be described. These aperture coupled devices are impedance matched for wideband operation. RF measurements show high gain and wideband operation for the devices and the results are in good agreement with that of simulation. The gain and bandwidth are determined to be 7.8 dBi and ~40% for a microstrip fed antenna device while they are 7.6 dBi and 38% for a CPW fed device.

3.1 Introduction to aperture coupled patch antenna

The design of microstrip antennas at microwave and millimeter wave frequencies is closely related to the feeding technique. At these frequencies, there are several problems such as feed dimensions, soldering of probes associated with the classical feeding techniques, such as coaxial probe (Fig 1 (c)) or edge feeds (Fig. 1 (a) and (b)). These considerations are even

more important for wideband applications, which require thicker substrates. On the other hand, the aperture coupled feeding technique (Fig. 1 (d)) has intrinsic properties which make it an attractive feature for millimeter wave applications. Wide-band operation of this type of microstrip fed antenna has been demonstrated at microwave and millimetre wave frequencies using either single or stacked patch configurations. Although all of the coupling methods depicted in Fig.1 have been shown to give excellent bandwidth characteristics, the indirect methods (Fig. 1 (b) and (d)) give rise to a high back-radiation level. However this is only true for aperture coupling (Fig. 1 (d)) if the aperture is near resonance. The aperture coupled antenna can also be fed with a CPW feed and is ideal at millimeter wave frequencies in the 30 GHz range (Mestdagh et al, 2004). It has been found that these antennas can easily be impedance-matched by tuning the dimensions of the excitation aperture and adding a small tuning stub.

Numerous advantages accrue for an aperture coupled configuration including those summarized previously (Pozar, 1985). They are listed below:

(i)   The configuration is suited for monolithic phased arrays, where active devices can be integrated on, for example, a gallium arsenide substrate with the feed network, and the radiating elements located on an adjacent (low dielectric constant) substrate, and coupled to the feed network through apertures in the ground plane separating the two substrates. The use of two substrates avoids the deleterious effect of a high-dielectric-constant substrate on the bandwidth and scan performance of a printed antenna array.
(ii)   No radiation from the feed network can interfere with the main radiation pattern, as the ground plane separates the two mechanisms.
(iii)   No direct connection is made to the antenna elements, so problems such as large probe self reactances or wide microstripline (relative to patch size), which are critical at millimetre-wave frequencies, are avoided.
(iv)   Ideal for micromachined antennas. The fabrication of a directly coupled feed probe would involve many fabrication steps.
(v)   The aperture coupled feeding technique has intrinsic properties which make it an attractive feature for millimeter wave applications.
(vi)   Wide-band operation of this type of microstrip antenna has been demonstrated at microwave frequencies (1 - 10 GHz) using either single or stacked patch configurations.
(vii)   A simple aperture coupled antenna structure gives rise to a high back-radiation level if the aperture is near resonance - this problem is eliminated by adopting a stacked antenna configuration.

A simple configuration of an aperture coupled microstrip antenna is shown in Fig. 1(d). It consists of a radiating patch on one substrate coupled to a microstripline feed on another parallel substrate, through an aperture in the intervening ground plane. It should be noted that the aperture coupled microstrip antenna can be used for both linear and circular polarizations. It requires two co-located orthogonal apertures each one excited by a different feed line. Each aperture excites orthogonal linearly polarized resonances under the normally square patch. The polarisation of the radiation from the patch is then dependent on the relative magnitude and relative phase of the signals entering the independent feed lines.

Circular polarisation is obtained when the signals are equal in magnitude and in quadrature phase.

For conventionally fed patch antennas (Fig. 1 (a) to (c)) it is well known that to a very good approximation the patch resonant frequency is dictated largely by the size and shape of the patch. This is not the case in aperture coupled patches. The aperture also has a resonant frequency and the coupled resonators formed by the aperture and the patch resonates at a frequency determined by simple filter theory. In this section a micromachined microstrip fed aperture coupled antenna is studied in depth. We then examine micromachined aperture coupled stacked antenna devices fed both from microstrip and CPW line. Antenna performances are assessed for various antenna configurations. Reflection coefficient (S_{11}), VSWR, normalise radiation pattern, gain, directivity and efficiency parameters are presented for a range of design parameters with the results plotted as a function of frequency as necessary. The effects of these different design parameters on the antenna performance are discussed.

3.2 Micromachined aperture coupled patch antenna
The gain and bandwidth of an aperture coupled antenna device can be significantly improved by introducing a micromachined air gap below the patch (see Fig. 2). These aperture coupled antenna devices which are described in ensuing sections are produced on a microwave PCB substrate. The air gap is achieved by suspending the patch on a micromachined polymer ring structure. A brief introduction to an established analytical design method is provided in order to communicate the fundamental operating principle of an aperture coupled antenna of the type described here. However, an electromagnetic field full-wave simulation software package is employed to design the antenna devices and adjust them for optimum performance. The effects of the design parameters, such as substrate material, air gap thickness, polymer rim dimensions and conductor materials, on the antenna's electromagnetic behaviour are investigated. The performances of several micromachined antenna devices are compared. Microstrip fed, CPW fed, single and stacked antenna configurations are included.

An aperture coupled antenna structure can be effectively modelled by means of a range of well established techniques. These are:

- Transmission line model (TLM)
- Finite element model (FEM)
- Finite difference time domain technique (FDTD)
- Method of moments technique (MOM)

All of these techniques exist in commercial packages. The general purpose modelling package, ANSOFT HFSS, is based on the finite element method, while CST Microstripes is based on the transmission-line matrix (TLM) method in time domain form. The IE3D package employs the method of moments. All are suitable for the kind of micromachined antenna devices described in this chapter. The antennas presented here are all modelled and optimised in the ANSOFT HFSS design environment.

The micromachined cavity-backed patch antenna design, realized by means of a polymer spacer, is quite similar to the strip-slot-form-inverted patch (SSFIP) antenna (Zürcher, 1988).

Fig. 2 shows a schematic of the cross-sectional and the top views of this potentially high gain, wide band antenna device. A square polymer ring (SU8 rim) mimics a sealed air filled cavity between the substrate and the polyimide thin film. The cavity-backed aperture coupled configuration improves radiation efficiency and thereby the gain of the antenna device. The configuration also improves the bandwidth of the antenna device owing to the proximity of the resonances of the coupling aperture and the patch.
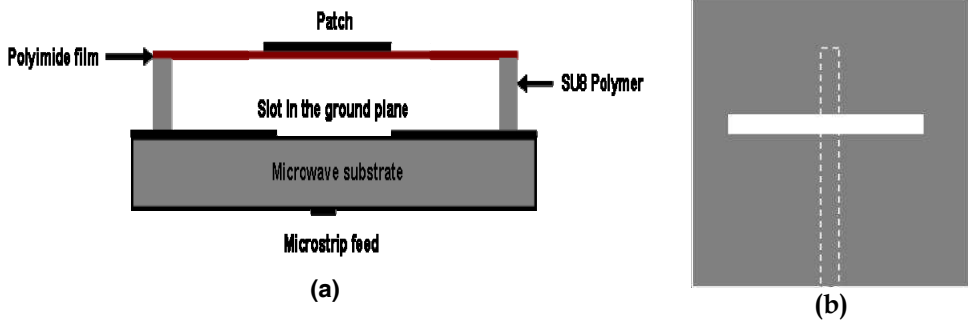

(a)

(b)

Fig. 2. Geometry of the (a) cross-sectional view and (b) top view of single patch micromachined aperture coupled antenna device.

The antenna centre frequency depends primarily on the dimensions of the resonant patch element and is given by

$$f_0 = \frac{c}{2 L_{eff} \sqrt{\varepsilon_{eff}}} \qquad (1)$$

where f_0 is the centre frequency of the antenna, c is the speed of light, L_{eff} is the effective length of the patch element and ε_{eff} is the effective dielectric constant. The device was designed to operate at around 12 GHz for ease of characterization using in-house measurement facilities. The design parameters such as the dimensions of the microstrip feed, aperture and top patch were optimized using the Ansoft HFSS electromagnetic simulation package with the aim of achieving high antenna radiation efficiency.

Parameter	Unit (mm)
Patch length	9.5
Patch width	11.5
Patch thickness	0.007
Slot length	11
Slot width	1.1
Microstrip length	18.84
Microstrip width	0.85
Inner length of cavity	19
Inner width of cavity	19
Cavity height	1.5
Thickness of polyimide film	0.125
Thickness of microwave PCB substrate	1.51

Table 1. Summary of the design parameters for the microstrip fed suspended patch antenna.

The height of the polymer rim was adjusted to obtain high gain. In the HFSS simulation, the lateral dimensions of the polymer rim were chosen to achieve high efficiency and compact size for the antenna structure. Table 1 summarizes the design parameters of the antenna device. A microwave PTFE material, AD300A, from Arlon MED (http://www.ctsind.com.sg/arlon.html), was used as the base substrate while a polyimide thin film (Du Pont) provided the supporting substrate for the suspended patch. The dielectric constant and loss tangent of the PTFE substrate are respectively 3 and 0.003. For the SU8 rim material they are 4.2 (Thorpe et al., 1998) and 0.042 (Lucyszyn, 2001) respectively, while the corresponding values for polyimide substrate material are 3.5 and 0.0026. In order to accurately model the performance of the antenna device, the parasitic effects of the SMA connector are simulated by introducing a short and wide rectangular extension at the input of the microstrip feed line. The dimensions (3mmx1.5mm) of the extension are chosen to match the length and diameter of the pin of the SMA connector. It has been observed that accommodating the effect of the connector is vital in order to accurately model the reflection characteristics of the suspended patch antenna. In the following sections the S_{11} parameters for estimating the bandwidth, normalised radiation pattern and radiation efficiency obtained from the HFSS designer environment are presented and discussed.

3.2.1 S parameters and study of the bandwidth
To assess the performance of the micromachined aperture coupled antenna device shown in Fig.2, the return loss (reflection coefficient in dB) and VSWR (voltage standing wave ratio) parameters are plotted for an optimum antenna, as in Fig. 3.
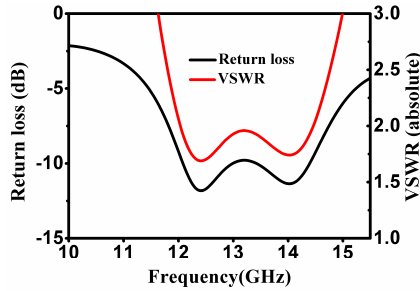
Fig. 3. Simulated return loss and the VSWR parameters for the optimized micromachined aperture coupled antenna device.

The return loss and VSWR parameters are plotted as a function of frequency from 10 to 15.5 GHz. It can be seen from the plot that the return loss is lower than -10 dB from around 12 GHz to 14.3 GHz and the VSWR is lower than a value of 2 in this range. Therefore the corresponding theoretical bandwidth of the antenna is 2.3 GHz or 17%.

3.2.2 3D antenna radiation pattern

The radiation pattern for the antenna device is obtained from the electromagnetic field solution and is plotted as a function of frequency from the far field plotter interface in Ansoft HFSS. Figure 4 shows the 2D and 3D far-field radiation patterns for the aperture coupled antenna device at 13.2 GHz near to the centre frequency of the operating band. The patterns show that there is high backward radiation and obvious side lobes in the E plane. But it will be shown in the later sections that the side lobes and back side radiation are reduced significantly using stacked patch configurations.
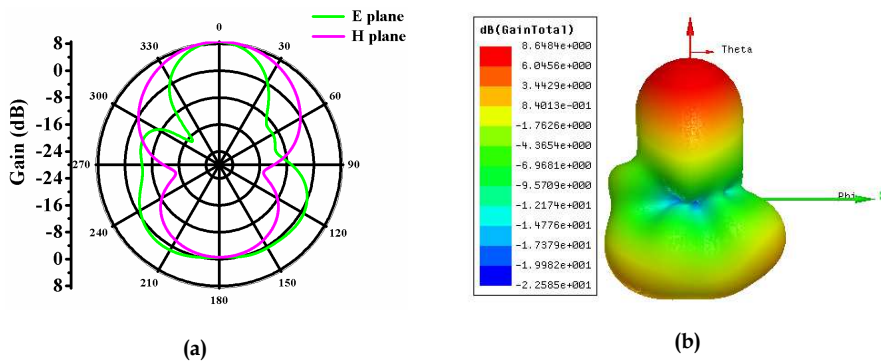

(a)

(b)

Fig. 4. 2D (a) and 3D (b) radiation patterns of a microstrip fed single patch antenna device at 13.2 GHz.

3.2.3 Directivity and gain

Fig.5 shows the variation of directivity, gain and efficiency for the microstrip fed aperture coupled antenna device with respect to frequency from 10 GHz to 15.5 GHz. The left 'y' axis gives the magnitude of antenna directivity and gain while the right 'y' axis gives the magnitude of absolute efficiency from 0.9 to 1. It can be easily seen from the plot the gain curve follows the directivity curve suggesting almost 100% radiation efficiency within the radiation bandwidth region. The gain varies from about 5 dBi at 10 GHz to around 8.3 dBi at 13 GHz and falls back below 6 dBi after 15.5 GHz. The excursions of directivity and gain within the radiation bandwidth (12 - 14.3 GHz) are below 1 dBi while it varies very significantly outside of this frequency range. The radiation efficiency varies from about 0.95 to close to 1 at 15.5 GHz. It should be noted that the radiation efficiency is a measure of total loss, including dielectric and conductor losses, within the micromachined antenna structure and it improves dramatically with the introduction of the micromachined air cavity.
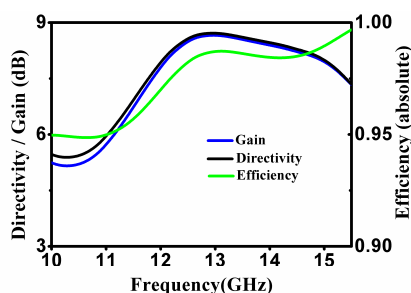

Fig. 5. Simulated gain, directivity and radiation efficiency for the optimized micromachined antenna device.

3.3 Stacked patch antenna devices

The design and modelling of the microstrip and CPW fed, stacked aperture coupled antenna devices is presented in the following sections. These stacked antenna devices are designed using a similar micromachined aperture coupled model as that presented in section 3.2. The stacked antenna configuration is exploited to further enhance the bandwidth and radiation pattern. The bandwidth is improved by utilizing the multiple closely resonant structures as well as through better impedance matching with the lower patch elements in the stacked configuration. The stacked patch elements are fabricated on polyimide substrates for microstrip fed devices and on LCP (liquid crystal polymer) film substrates for the CPW configurations, supported, in all cases, by the micromachined SU8 polymer spacers

3.3.1 Microstrip fed aperture coupled stacked patch antenna

3.3.1.1 Antenna Design

 Stacked, cavity backed, aperture coupled antenna geometries have been modelled using Ansoft HFSS and optimized. Fig. 6(a) provides a cross sectional view of a microstrip fed stacked antenna of the type described in this section, while the top view of the coupling aperture on the lower microstrip substrate surface is depicted in Fig. 6(b). The arrangement consists of a double cladded microwave PTFE substrate, and two suspended patches to form

a stacked antenna device. The microstrip feed line on the bottom surface of the microwave substrate excites the lower patch through a rectangular coupling aperture in the ground plane which forms the top surface of the microwave substrate. The patch elements are printed on thin film (polyimide) substrates. They are supported by micromachined polymer spacers to reduce the antenna loss and hence to improve its gain. The cavities are sealed by the bonded polymer rings thus providing protection against the incursion of moisture and particles, which could contribute unwanted losses.

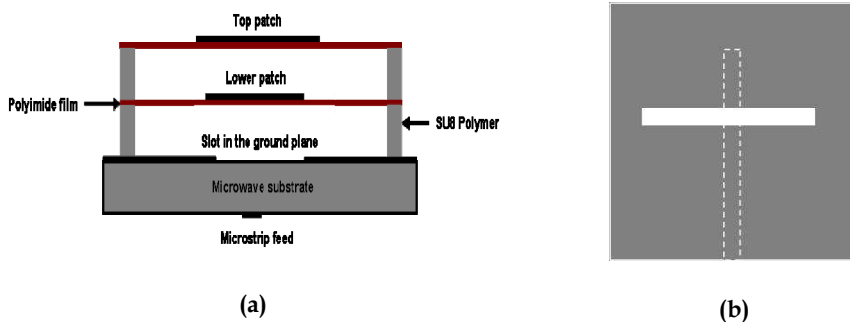**(a)**   **(b)**

Fig. 6. (a) Schematic cross-sectional view of the stacked microstrip fed aperture coupled antenna using micromachined polymer spacers, (b) The top view of the aperture and feed line on the substrate surfaces.

Parameter	Microstrip fed device (mm)	CPW fed device (mm)
Lower patch length	5.8	9.4
Lower patch width	9	18
Upper patch length	9.6	12.6
Upper patch width	10.6	18
Patch thickness	0.009	0.009
Slot length	9.8	16.5
Slot width	0.98	1.6
Microstrip length	15.00	18.2
Microstrip width	0.82	1.4
Inner length of cavity	19	18.2
Inner width of cavity	19	18.2
Lower cavity height	2.2	1.0
Thickness of polymer rim	1.0	1.0
Upper cavity height	0.67	1.0

Table 2. Summary of the design parameters for the suspended stacked patch antennas

The stacked antenna has been designed using a similar approach to that described previously for the development of multi-layer stacked wideband antenna devices (Pavuluri et al., 2008, Wang and Pavuluri, 2008, Croq and Pozar, 1991). It is designed for operation at

X-band (8 – 12 GHz) with a 40% of bandwidth. The height of the air cavities formed by the micromachined polymer rims located between each stacked patch and the substrate, is adjusted for optimum bandwidth while at the same time maintaining a low profile for the overall antenna structure. For this microstrip fed device, the top patch and the aperture are dimensionally adjusted to ensure resonance at similar frequencies, while the dimensions of the microstrip line and the lower patch are tuned to secure the best possible impedance match. In the design process the initial dimensions of the patches are determined by the choice of the center frequency of operation. The width of the coupling aperture is conventionally set at about 10% of its length.

The heights of the air cavities as explained earlier are a trade-off between the desire for bandwidth and the limitations set by the fabrication process. The length of the feedline is then varied to obtain sufficient bandwidth. In order to obtain fixed band performance, the lengths of the top patch and the aperture are modified to tune the band of operation. Fine impedance tuning is achieved by adjusting the dimensions of the lower patch. The shape and dimensions of the SU8 spacer rings are chosen carefully to ensure good antenna performance. It is generally necessary to carry out several iterations of the above steps to obtain an acceptable antenna delivering high gain and wide bandwidth. The optimized design parameters are given in Table 2.

3.3.1.2 S parameters and study of the bandwidth

To determine the predicted performance of the optimally designed aperture coupled antenna, the return loss and VSWR are plotted as a function of frequency. The plot width at the -10 dB return loss locations as in Fig.7, quantifies the bandwidth. From the plot the return loss is lower than -10 dB from about 7.8 GHz to 12 GHz. The VSWR is lower than a value of 2 over this range. Therefore the theoretical bandwidth of this device is 4.2 GHz or 42%. This is an improvement of a factor of 2.5 over that of the single patch device.
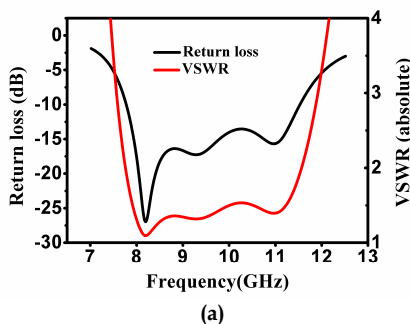

(a)

Fig. 7. Simulated insertion loss and VSWR parameters for the optimized micromachined microstrip fed stacked aperture coupled antenna.

3.3.1.3 3D antenna radiation pattern

The radiation pattern for the antenna device is obtained from the electromagnetic field solution and is plotted as a function of frequency using the far field plotter interface in Ansoft HFSS. Figure 8 shows the 2D and 3D far-field patterns for the aperture coupled

antenna device at 9.82 GHz near to the centre frequency (9.9 GHz) of the operating band. It can be seen that the back side radiation is reduced to around -4 dB for the microstrip fed stacked patch antenna configuration.
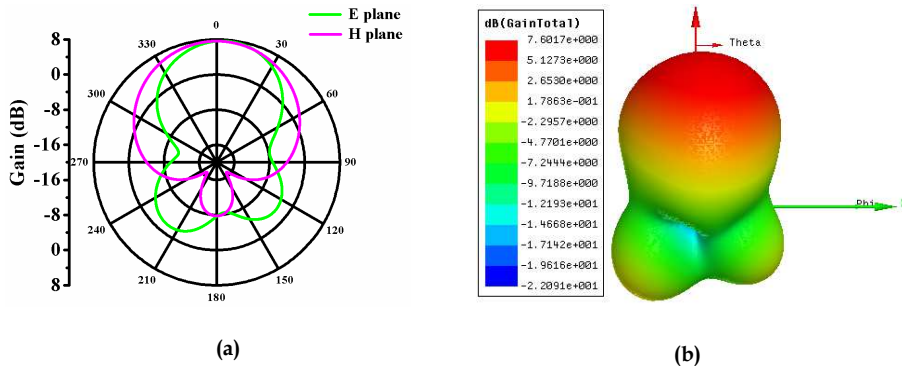

(a)   (b)

Fig. 8. 2D (a) and 3D (b) radiation patterns at 9.82 GHz.

3.3.1.4 Directivity and gain

Fig. 9 shows the dependence of directivity, gain and efficiency on frequency, in the range from 7 GHz to 12 GHz, for the microstrip fed stacked antenna. The results are not too dissimilar to those of the single patch antenna (Fig. 4), but with less gain and efficiency variation over the optimum operating band. The gain and directivity vary from about 6 dBi at 8 GHz to around 7.8 dBi at 9.7 GHz and falls back below 6 dBi after 12.5 GHz. The directivity and gain are constant to within 2 dBi over the previously defined -10dB bandwidth. Outside this bandwidth gain diminishes significantly. The radiation efficiency is greater than 0.95 from 8 GHz to 12 GHz.
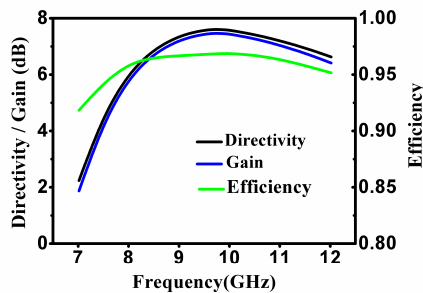

Fig. 9. Simulated gain, directivity and radiation efficiency of the optimized micromachined microstrip fed stacked aperture coupled antenna.

3.3.2 CPW-fed aperture coupled micromachined patch antenna

An antenna comprising three stacked patches fed from a coplanar waveguide (CPW) has also been studied. Fig. 10 show the schematics of the CPW fed stacked patch antenna. A single cladded PTFE substrate (Taconic TLY-3-0200-CH/CH) was used to support the CPW line and the coupling aperture. The stacked patches are suspended symmetrically above the

aperture using micromachined SU8 polymer rims. As the air gap between the base microwave substrate (Fig. 10(a)) and the lowest patch is smaller than that of the microstrip fed stacked device (Fig. 6(a)) for ease of fabrication, an additional patch is required to yield a similar bandwidth of ~40%. The upper pair of patches has the same dimensions and it is the electromagnetic coupling between them that further increases the bandwidth of the antenna. The coupling slot on the ground plane and the top two patches were designed to be in close resonance. The bottom patch and the λ/4 stub are optimized for a wide 'match' bandwidth. Tables 2 and 3 show the physical dimensions of the structure layers for the antenna device.
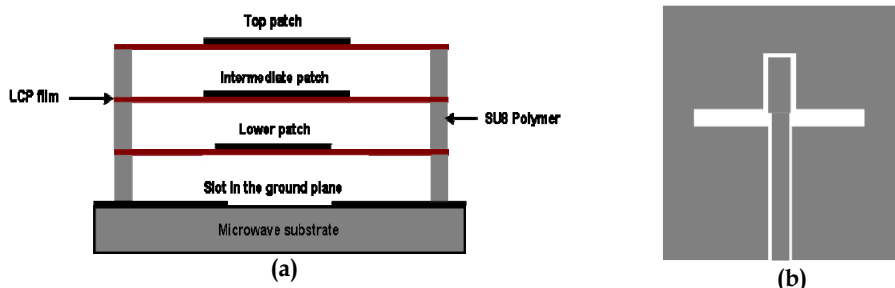

(a)   **(b)**

Fig. 10. (a) Cross-sectional view of the stacked CPW fed antenna using micromachined polymer spacers, (b) top view of the corresponding aperture and feed line on the substrate surface.

Substrate	Thickness (mm)	Dielectric constant	Loss tangent
Taconic PTFE substrate	0.5	2.2	0.0009
LCP film	0.10	3.2 (Thompson et al., 2004)	0.002

Table 3. The thickness and microwave property of Taconic PTFE and LCP substrates.
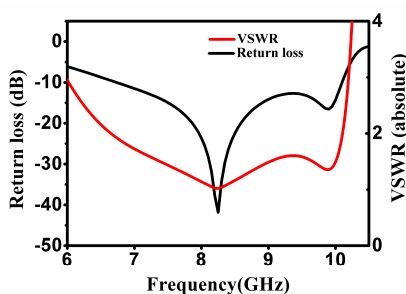

Fig. 11. Simulated insertion loss and VSWR parameters for the optimized micromachined CPW fed stacked aperture coupled antenna.

3.3.2.1 S parameters and study of the bandwidth

The return loss and VSWR parameters are plotted as a function of frequency from 6 to 10.5 GHz in Fig.11. It can be seen from the plot that the return loss is lower than -10 dB from

around 6.5 GHz to about 10.2 GHz, and the VSWR is lower than a value of 2 over this range. The corresponding theoretical bandwidth is 44%.

3.3.2.2 Radiation pattern and gain

As with earlier examples, the radiation pattern for the antenna device is obtained from the electromagnetic field solution. It is plotted at a given frequency using the far-field plotter interface in Ansoft HFSS. Fig. 12 shows the 2D and 3D far field patterns for the aperture coupled triple patch antenna device at 8.3 GHz. It can be seen that the back side radiation is reduced to around -7 dB in the E and H plane radiation characteristics. The backward radiation is significantly less than that of the microstrip fed devices. The reduction of the back radiation can be attributed to the effect of the CPW based feeding method. Thus the CPW feeding approach is recommended for minimal backward radiation.
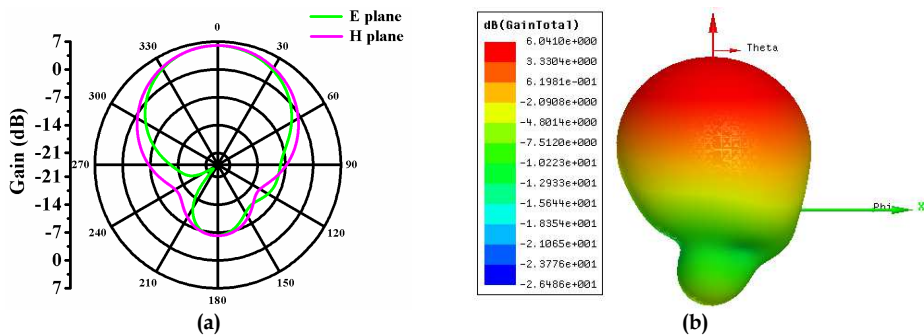

(a)   (b)

Fig. 12. 2D (a) and 3D (b) radiation patterns for the CPW fed stacked antenna at 8.3 GHz.

3.3.3 The effect of polymer rim design on the performance of the CPW fed stacked aperture coupled antenna

As stated previously the SU8 polymer has high dielectric loss at microwave frequencies with a loss tangent of 0.043. The effect of the dimensions of the polymer rim on antenna performance has been studied using the CPW fed antenna design. Two rim designs of 23mmx23mm and 12.5mmx18mm are used and the corresponding projected views of the antennas are shown in Fig. 13. The other design parameters remain the same as shown in Table 2. Fig. 14 shows the efficiency of the CPW fed stacked antenna device for the two polymer rim designs in the frequency range of 6.5 GHz to 10.5 GHz. As can be seen from Fig. 14 the efficiency of the antenna device for the larger rim is greater than 0.95 from 6.5 GHz to 10.5 GHz but it is less than 0.9 with the smaller polymer rim. It can also be seen that the roll-off rate of the antenna efficiency above 9.5 GHz is much faster for the smaller rim indicating rapid decrease of the antenna performance.

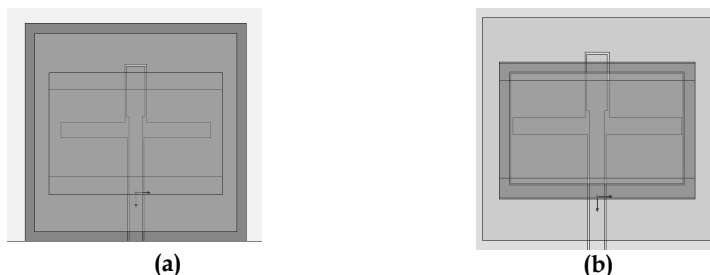**(a)**   **(b)**

Fig. 13. A 3D view of the optimized micromachined CPW fed stacked aperture coupled antenna with two different polymer rim dimensions.
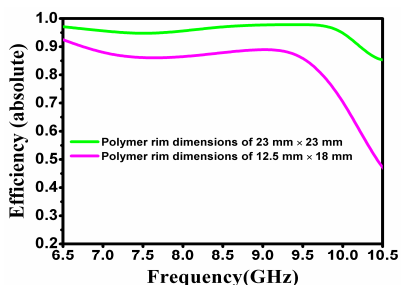

Fig. 14. Results of antenna efficiency of the CPW fed antenna for different SU8 polymer rim dimensions

3.3.4 Effect of the substrate loss

As the losses in the substrate layers in a stacked antenna affects its performance significantly, for comparison, FR4 and PTFE based stacked CPW antenna designs with similar dimensions as that of the CPW antenna shown in Fig. 10 are also designed and optimized for impedance matched performance. These two devices consist of 4 layers of FR4 or PTFE material with 3 three stacked patches. The dielectric constant and the loss tangent for the FR4 material are taken as 4.2 and 0.020 respectively (Aguilar et al., 1998). Fig. 15 shows the efficiency and gain as a function of frequency for the three CPW fed stacked antenna configurations. The rapid decrease of gain above 9 GHz of the FR4 based device is due to the increased insertion loss as the frequency is out of the band of operation. The gain of the antennas was obtained from the simulation results of the radiation characteristics. It can be seen that there is little difference between gain values of the stacked patch antenna based on the multilayer PTFE structure and the devices with suspended patch elements since the dielectric loss is minimal in both cases. However, the micromachined device has a larger bandwidth. The performance of the FR4 based multilayer antenna is much poorer due to the well known lossy behaviour of the FR4 material beyond the microwave frequency region. Table 4 gives a summary of the performance parameters. The micromachined antenna device with suspended patches showed the best bandwidth of about 38% close to that required for ultra-wide band applications.

Thank You for previewing this eBook

You can read the full version of this eBook in different formats:

- ➤ HTML (Free /Available to everyone)

- ➤ PDF / TXT (Available to V.I.P. members. Free Standard members can access up to 5 PDF/TXT eBooks per month each month)

- ➤ Epub & Mobipocket (Exclusive to V.I.P. members)

To download this full book, simply select the format you desire below